Supplementary Information

H. Jönsson, M. Heisler, G.V. Reddy, V. Agrawal, V. Gor, B.E. Shapiro, E. Mjolsness and E.M. Meyerowitz

Modeling the organization of the WUSCHEL expression domain in the shoot apical meristem

Bioinformatics **21** (Suppl. 1), i232-i240 (2005)

Additional results

Additional ablation experiment simulation

In the paper we emulate the laser ablation experiment by simulating the models on a lattice where the central cells are removed. The activator model created two stable WUS domains at opposite sides of the ablated region where an intermediate time point showed a weak WUS expression around the ablated region (Figure 7E-F in the paper). This is in full agreement with experiments, but in the experiments also plants with a single new WUS region appeared. The activator model can produce this behavior as well, using a slightly different set of parameters. Figure 1 show a simulation where the diffusion rates for A and B are increased, leading to a dynamics with a somewhat larger distance between potential peaks. In this case, the model starts as before creating a weakly expressing region surrounding the ablated region, but the equilibrium expression is within a single peak at the side of the ablated region.

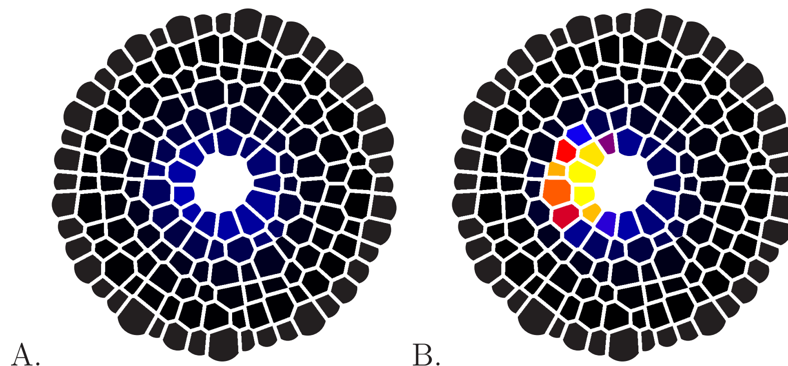

Figure 1: Simulation emulating the laser ablation experiment using the activator model with $D_a = 0.15, D_b = 2.25$ and other parameters as in Table 1 in the paper. A) Early time point. B) Equilibrium time point.

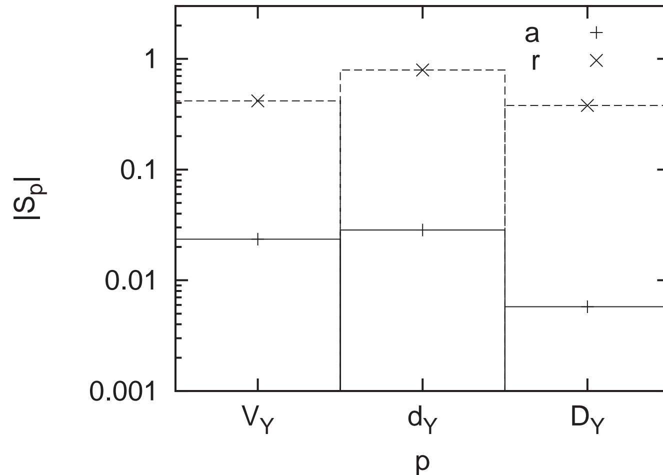

Figure 2: Absolute values of the sensitivity S_p for the parameters D_y, V_y, and d_y. Values are presented for both models (a: activator model, r: repressor model). We have used a parameter perturbation, $f = 1\%$ for this analysis.

Sensitivity analysis

As discussed in the paper, the interaction network controlling SAM development is highly robust. This should be reflected in models as well, and we here present a local sensitivity measure to investigate the relative change in WUSCHEL concentration due to changes in parameter values. We use the sensitivity measure S_p defined by

$$S_p = \frac{dC}{dp}\frac{p}{C} \approx \frac{\Delta C}{\Delta p}\frac{p}{C} = \frac{1}{f}\frac{C\left(p+\Delta p\right) - C\left(p\right)}{C(p)}, \tag{1}$$

where

$$C = \sum_{cell}^{N_{cell}} C_{WUS}^{cell} \tag{2}$$

is the total WUSCHEL concentration (while N_{cell} is the number of cells and C_{WUS}^{cell} is the cellular concentration). p is the parameter that is changed a fraction f ($\Delta p = fp$).

We concentrate on how sensitive the WUSCHEL expression is to small changes in the repressing signal Y, i.e. how accurate does this signal have to be to get a distinct WUS region as seen in experiments. We investigate this by calculating sensitivities for the parameters that determine the strength and shape of the signal Y. In both models, Y shape and strength are determined by V_y, d_y, and D_y (in Equations 5-10 in the paper), and the absolute values of S_p for these parameters can be found in Figure 2. As can be seen, the activator model shows a higher robustness in these parameters; typically it has an order of magnitude lower S_p. This shows a beneficial feature of having a patterned activator. The model can create a well defined WUSCHEL region less dependent on the exact behavior of the repressing signal. On the other hand, the "threshold" type of model

that is represented by the repressor model is more dependent of the strength and shape of the Y signal. These features solely determine which cells that are above or below the threshold value, and hence determine the activity of the WUSCHEL production.

This robustness is an interesting property of the activator model, but as noted in the paper, the model is only a part of the feedback mechanism regulating the *CLV3* and *WUS* expression regions and to make any conclusion the sensitivity should be measured in a model where also the activation of CLV3 by a WUS originating signal is included.

Template statistics

The image processing techniques allows for the extraction of various quantitative features of the cells in the experimental template. In the paper we show the extracted pWUS::GFP plotted on the template (Figure 3D in the paper), but also spacial and topological properties can be extracted and we here present some examples. In Figure 3A the distribution of cell sizes (areas) is shown, and it can be seen that the total size range is quite large. The number of cell neighbors are centered around 5-6 neighbors (Figure 3B), where the cells with low number typically belongs to the outer layer of cells (L1). In the distribution of pWUS::GFP intensities (Figure 3C) it can be seen that most cells have a low expression while there are a few cells (in the centered peak) with high expression.

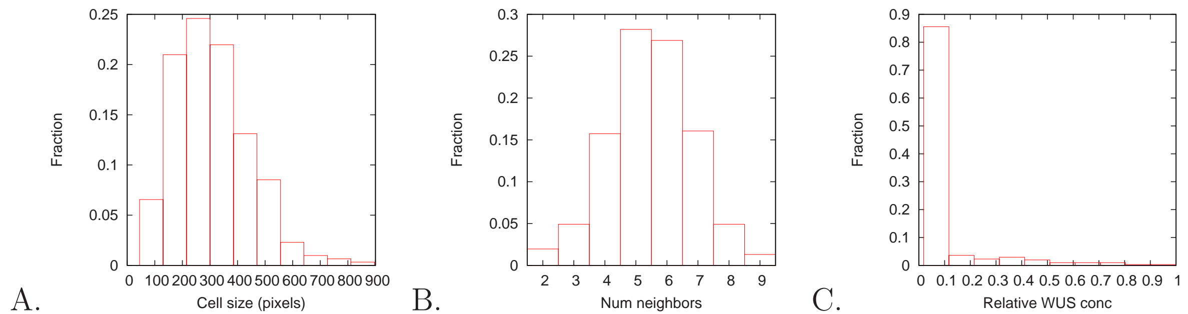

Figure 3: Statistics from the two-dimensional experimental template (Figure 3 in the paper). A) Size distribution of the extracted cell compartments measured in pixels (1 pixel $= 0.15 \times 0.15\ \mu m^2$). B) Distribution of the number of neighbors for the extracted cell compartments. C) Relative WUS intensities in the cells, interpreted as WUS expression or concentration.

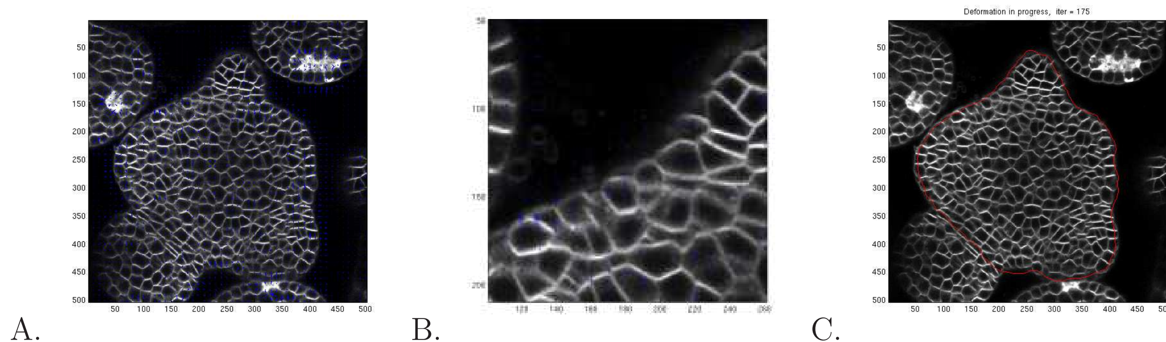

Figure 4: Snake algorithm working on a GVF field. A) The gradient vector flow field for the complete image. B) Magnification of the GVF on a boundary region. C) The resulting snake.

Image processing

Background extraction

Since the cell extraction algorithm looks for dark regions in the image, the dark background (non-merisem tissue) needs to be removed. This is done using a snake algorithm working on a gradient vector flow field (GVF) on the membrane picture (ref Xu and Prince, 1998 in our paper). We use the matlab GVF package as provided at http://iacl.ece.jhu.edu/projects/gvf/ and refer to the reference and documentation available for a more detailed description, and we use the same synntax as in the reference here.

Assume a grey-scale image with intensities $I(x, y)$, where x, y are the rows,columns of the image. A snake is a parameterized curve, $(x(s), y(s))$ in the image that can be used to find edges in an image. In the GVF formulation it can be defined as satisfying a force balance equation $F_{int} + F_{ext} = 0$, where F_{int} is an internal force of the curve discouraging streching and bending, while F_{ext} is an external force defined by properties of the image. The GVF-snake uses a gradient vector flow field as the external force ($F_{ext} = \mathbf{v}(x, y) = [u(x, y), v(x, y)]$). We use parameters $\alpha = 1, \beta = 1, \mu = 0.1$ and the edge map $f(x, y) = | \div I(x, y)|^2$ (as defined in Xu and Prince, 1998), resulting in a GVF field as shown in Figure 4A,B. The snake is initiated by clicking around the SAM, and the imortant feature for the algorithm to work is that the GVF field points towards the SAM in the surrounding background (Figure 4). The resulting snake is shown in Figure 4C which is to be compared with Figure 3B in the paper.

Cell compartments extraction

Cells compartments are extracted from the membrane picture using a watershed algorithm. The algorithm starts in each pixel, and walks downhill in the "intensity landscape" until it reaches a minimum. All pixels that end up in a single minimum are regarded as one cell. A picture of the borders of the extracted cells can be seen in Figure ??C. A beneficial feature of this algorithm is that it is easy to extract neighborhood relations, including the length of the "wall" connecting two neighbors. Included in this algorithm is a preprocessor reducing noise by a simple region averaging.

Concentration extraction

Finally we use the cell compartment information extracted from the membrane picture to extract average intensities for these compartments (I_c) in the pWUS::GFP image.

$$I_c = \frac{1}{N_p} \sum_{p}^{N_p} I_p^{(WUS)}, \tag{3}$$

where the summation is over the N_p pixels p defining the compartment, and $I_p^{(WUS)}$ is the pixel intensity in the pWUS::GFP image. These numbers are interpreted as relative expression/concentration values.